Journal of Applied Mechanics and Technical Physics, Vol. 42, No. 4, pp. 672–679, 2001

OSCILLATION OF THE ELEMENTS OF COMBUSTIBLE FOREST MATERIALS AND ITS EFFECT ON IGNITION AND COMBUSTION

A. M. Grishin,[1] A. N. Golovanov,[1] and V. V. Medvedev[2]

UDC 536.24

Oscillations of the elements of combustible forest materials in a laminar air flow were studied experimentally using optoelectronic equipment. The values of the Young's modulus and rigidity are found to agree well with the available data. It is shown that interaction of the elements of combustible forest materials with air flows leads to asymmetric separation of the flow, which makes needles and twigs oscillate at frequencies comparable to the frequencies of their natural oscillations. An analysis of the experimental data gives limiting values for the equilibrium wind speed in a forest canopy for which forest fires can arise or extinguish.

In forest fires, combustible forest materials (CFM) is known to burn in a diffusion regime [1]. Therefore, the oscillation mechanisms and the effect of oscillations of the CFM elements (thin twigs and needles) on the heat- and mass-exchange coefficients are of considerable interest.

Grishin [1, 2] proposed a hypothesis on the oscillation mechanism of the CFM elements and their effect on CFM combustion. According to this hypothesis, oscillations of the CFM elements in a forest canopy are due to asymmetric separation of a gas flow from the surface of an CFM element. As a result, the combustion regime changes, and an upper forest fire can ultimately arise. In the present work, we confirm experimentally this hypothesis, propose an approximate method for determining the oscillation frequency of CFM, and study the effect of heat and mass exchange on the ignition and combustion regimes of CFM.

1. Goals and Experimental Methods. The main goals of this work is to study experimentally oscillations of typical CFM elements in a gas flow, determine oscillation frequencies and elastic properties of CFM, analyze the effect of these oscillations on the ignition and combustion regimes, and determine the critical wind speed at which an upper forest fire can arise.

From the viewpoint of mechanics, any tree is a complex structure that includes the following elastic elements: trunk, branches, thin twigs located on the branches, and needles located on the thin twigs. Each element of this structure has a natural frequency. Since needles and thin twigs constitute about 70% of all CFM elements, we studied oscillations of these elastic bodies. The physical model for these bodies was a cantilever — a beam which is fixed at one end and the other end is free. We note that although a real needle is curved, the maximum degree of its curvature $\Delta x_{\max}$ is negligible compared to its length l_s. Thus, a needle can be treated as a straight cylinder with effective diameter $d_s = 2\sqrt{s/\pi}$, where s is the middle cross-sectional area. Twigs are straight round cylinders. In addition, we considered the flow around a twig with an aggregation of needles. Figure 1 shows diagrams of the experiments. We note that cross sections of twigs are circles, and cross sections of a pine needle have a complicated crescent form [1].

Figure 2 shows a photograph of a needle cross section with 20-fold magnification. The moisture content of a needle is $W = (m - m_0)/m_0 = 67.8\%$, where m and m_0 are the masses of a wet needle and a needle dried, respectively, at a temperature $T = 100°$C. The CFM elements were placed in the operating section of the MT-324 subsonic wind tunnel of the Tomsk State University. Arrows in Fig. 1 show the directions of the laminar air flow

[1]Tomsk State University, Tomsk 634050. [2]Tomsk State Polytechnical University, Tomsk 634004. Translated from Prikladnaya Mekhanika i Tekhnicheskaya Fizika, Vol. 42, No. 4, pp. 127–135, July–August, 2001. Original article submitted January 12, 2001.

 0021-8944/01/4204-0672 $25.00

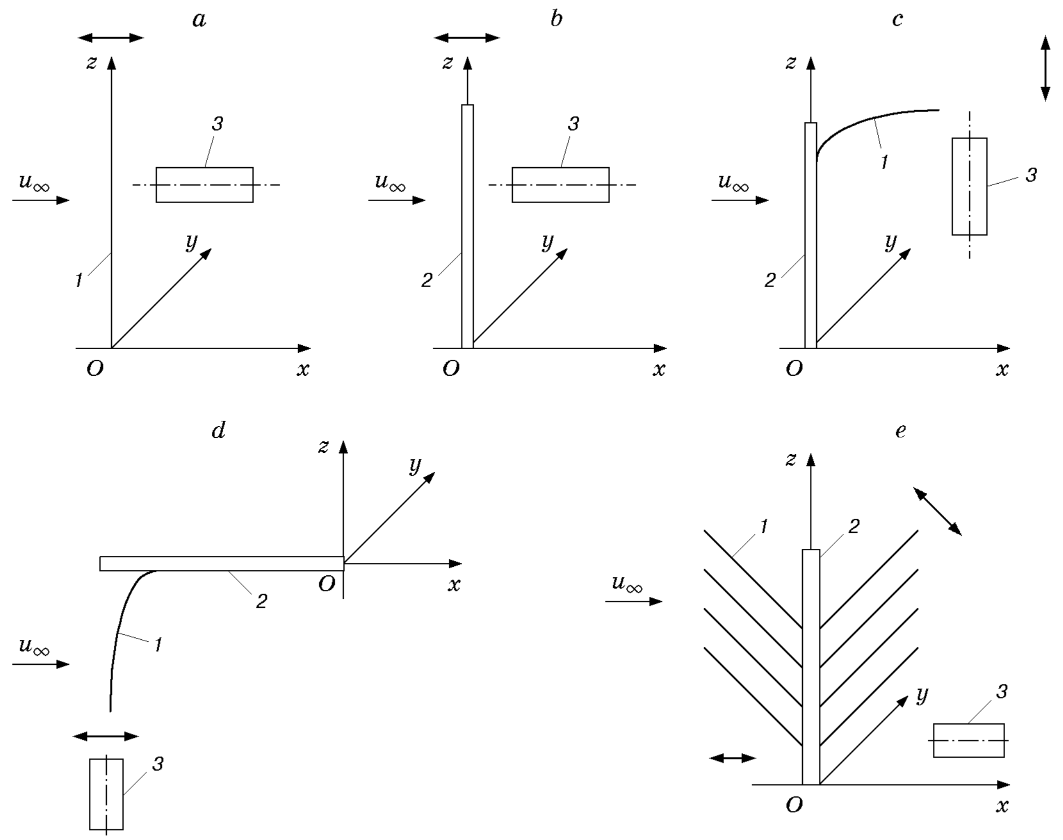

Fig. 1. Schematic arrangement of the CFM elements: pine needle (1), twig (2), and optoelectronic sensor (3); (a) flow around a single needle; (b) flow around a thin twig; (c and d) flow along and across "twig–needle" cantilevers; (e) flow around a twig with needles.

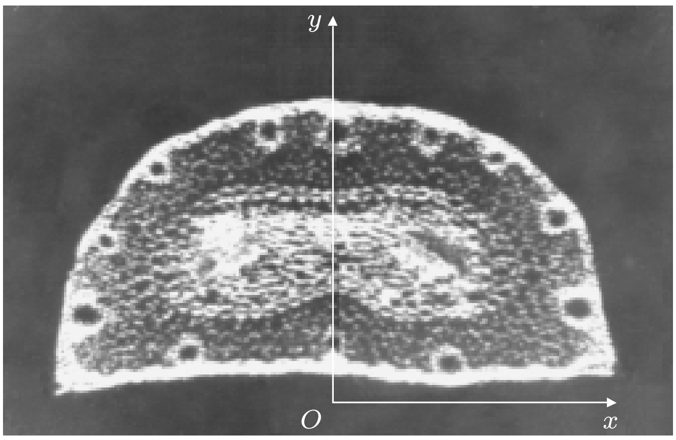

Fig. 2. Cross section of a needle and the coordinate axes chosen to determine the moment of inertia.

velocity u_∞. The flow rate measured with a Pitot–Prandtl air-speed head and a heat loss anemometer [3] varied within $u_\infty = 1.0$–3.6 m/sec. The air flow generated periodic oscillations of needles 1 and twigs 2 (see Fig. 2) in the xz and yz planes (thick arrows show the displacement x from the equilibrium position). The z axis is directed upright from the fixed end of the cantilever. The displacement x and the oscillation frequency f were measured with a fiber-optic sensor (3), which recorded oscillations in the xz and yz planes. The sensor consisted of two crystal-polymeric light guides each 0.3 mm in diameter, whose free ends were joined together and placed at distance h from the needle that reflected light diffusively. The light from an MN 6.3-0.3 incandescent lamp was incident on the end of one of the guides and further transmitted onto the needle surface. The reflected light beam passed

TABLE 1

CFM element	l_s, mm	d_s, mm	W, %	f, Hz
Pine needle	26	0.7	11.2	20.0
Pine needle	41	0.9	19.1	21.4
Pine needle	43	1.0	54.2	16.7
Cedar needle	80	1.0	12.1	38.5
Fir needle	16	0.7	12.7	4.4
Pine needle	60	4.0	—	21.0

TABLE 2

u_∞,	Pine needle*				Pine twig**			
m/sec	f, Hz	A, mm	Re	Sh, 10^{-3}	f, Hz	A, mm	Re	Sh, 10^{-3}
1.1	20–26	1.15	68.3	18.0	2.1	0.10	100.5	7.6
1.6	18–22	1.56	99.3	12.4	2.0	0.12	436.9	5.0
1.9	18–22	1.74	117.3	10.4	2.1	0.13	518.8	4.4
2.5	20–25	1.91	155.3	7.9	2.0	0.14	682.9	3.2
3.1	20–26	2.07	192.3	6.4	2.1	0.16	846.6	2.7
3.6	20–25	2.20	223.3	5.5	2.1	0.17	983.0	2.3

One asterisk indicates that $l_s = 41$ mm, $d_s = 0.9$ mm, and $W = 19.9\%$; two asterisks indicate that $l_s = 60$ mm and $d_s = 4$ mm.

through the other light guide to the window of an FÉU-118 photodetector, where it was converted to an electric signal and recorded by an oscillograph as a function of time t and the distance h. Before each series of experiments, the value of h was calibrated using a micrometer table.

The time resolution of the sensor is $\tau = R_{\rm load}C_{\rm ph} = 10^{-6}$ sec ($R_{\rm load} = 100$ kΩ is the load resistance and $C_{\rm ph} = 10^{-10}$ F is the interdynode capacity of the FÉU-118 photodetector). The space resolution of the sensor is 1 mV/μm.

The experiments were conducted with typical CFM elements (twigs and needles). In a sample, the mass of thin twigs is $m = 0.25$–0.30 g and the mass of a needle is $m = 0.012$–0.020 g; the length of a needle is $l_s = 45$–55 mm and the length of a twig is $l_s = 40$–70 mm; the twigs were 3.5–7.0 mm in diameter and the equivalent diameter of needles was 0.95–1.09 mm.

2. Experimental Results of Studying Natural Oscillations of a Single Needle and a Bald Thin Twig in Immobile Gas and a Laminar Air Flow. At the first stage of experiments, we compared the natural frequencies of oscillations of single needles and twigs (see Fig. 1a and b) generated by a solitary perturbation with an amplitude $A_0 = 2$ mm (Table 1) and a continuous perturbation of amplitude A produced by an air flow in the wind tunnel (see Table 2, where Re is the Reynolds number and $\mathrm{Sh} = fd_s/u_\infty$ is the Strouchal number).

Figure 3a and b shows oscillograms of the oscillation amplitude as a functions of time under the solitary perturbations (damped oscillations) and in the air flow (continuous oscillations close to harmonic oscillations).

The variation of the initial oscillation amplitude $A_0 = 0.5$–4.5 mm due to the initial perturbation did not change the natural frequencies of the CFM elements. We note that the natural frequencies of pine needles depend slightly on the moisture content (see Table 1). For a pine needle, $f = 21.4$ Hz at $W = 19.1\%$ and $f = 16.7$ Hz at $W = 54.2\%$. For the frequency range considered, the oscillation frequencies of pine needles in the air flow do not depend on the wind speed and coincide with the oscillation frequencies in still air (see Table 2).

3. Mechanism of Flow around Needles and Thin Twigs. It is known that flow around heat exchanger pipes can lead to aerodynamic vibrations of the pipes due to asymmetric separation of the flow [4, 5]. In this case, a portion of the flow energy is spent to maintain pipe vibrations at frequencies close to the natural frequencies of elastic oscillations. In laminar flow around a cylinder at Reynolds number $\mathrm{Re} = \rho u_\infty d/\mu > 60$, a vortex trail appears, which is called a Kármán vortex trail [5]. Vortex trails can generate acoustic noise and cause oscillations of CFM [1]. In our experiments, the air flow Reynolds number was varied within $50 \leqslant \mathrm{Re} \leqslant 400$. The possible frequencies of vortex separation were calculated by the formula $f_n = \mathrm{Sh}_* u_\infty/d_s$ ($\mathrm{Sh}_* = 0.2$ [1, 4]) and are given in Table 3.

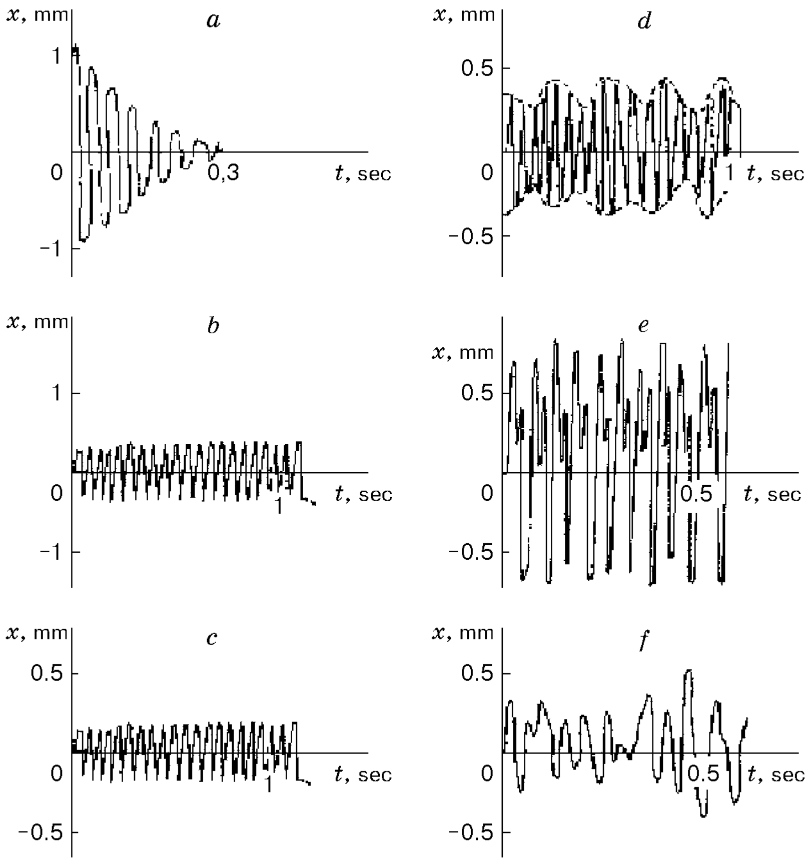

Fig. 3. Oscillograms of CFM oscillations under solitary perturbation (a) and in the air flow (b–f): oscillogram (a) refers to the diagram in Fig.1a; oscillograms (b) and (c) refer to the diagrams in Fig. 1b (along the Ox and Oy axis, respectively), and oscillograms (d), (e), and (f) refer to the diagrams in Fig. 1c, d, and e, respectively.

Figure 4 shows a photograph of the gas flow behind a needle (light vertical line on the right side of the photograph) that corresponds to the diagram in Fig. 1a. A drop of oil placed on an electrically heated wire produced a plume of smoke, which flew around the needle. The photograph shows plumes from four drops. Oscillations gave rise to periodically changing dark and light spots in the plumes. The light spots appeared in the photographs at a frequency of $f \approx 20$ Hz, which coincides with the oscillation frequencies of needles. The asymmetric change of dark and light spots in the photograph indicates asymmetric separation of the gas stream during flow around the CFM elements.

Twigs and needles oscillated not only in the xz plane (see Fig. 2) but also in the zy plane. The frequencies of oscillation in the zy plane coincided with the frequencies of oscillation in the xz plane, and the amplitude for the studied flow rates was equal to 0.17–0.30 values of the oscillation amplitude in the xz plane. This indicates that the oscillations of needles and thin twigs are due to asymmetric separation of the laminar flow [1, 4].

Figure 3f shows the x coordinate of a needle versus time for the flow around a twig with needles according to the diagram in Fig. 1e ($u_\infty = 1.1$ m/sec). Obviously, these oscillations are superpositions of oscillations of the needle and the twig.

4. Determining the Elastic Properties of the CFM Elements. Data on the natural frequencies of the CFM elements can be used to determine the elastic properties such as effective Young's modulus E and rigidity EI (I is the moment of inertia). The values of E and EI were calculated by the formulas [1, 6, 7] for the minimum natural frequency of a cylindrical cantilever:

$$f_s = \frac{3.52}{l_s^2}\sqrt{\frac{EI}{m_l}}, \qquad m_l = \frac{m}{l_s}, \qquad I = \frac{\pi d^4}{32}. \tag{1}$$

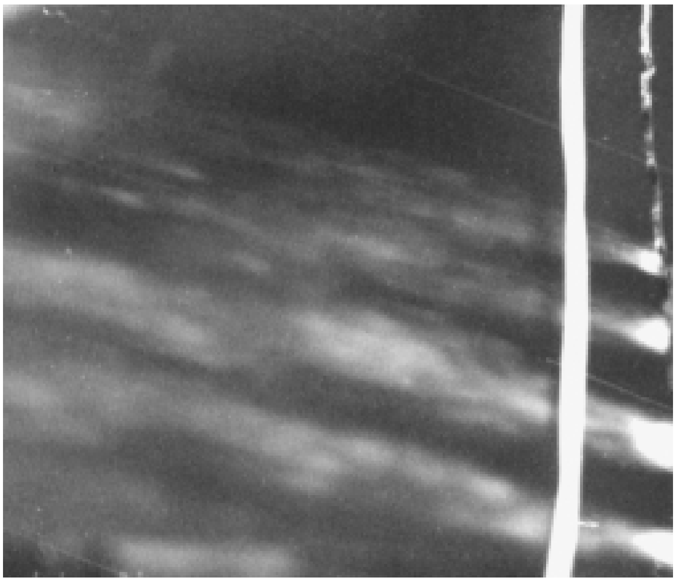

Fig. 4. Plume of heated oil drops after a needle.

TABLE 3

CFM element	Re	f_n, Hz	
		Fig. 1c	Fig. 1d
Twig	259	6286	—
	375	9143	—
	445	10 858	—
Needle	74	—	32,000

In the calculations, the moment of inertia of an actual needle was replaced by the moment of inertia of an effective cylinder with radius $r_{\rm eff} = \sqrt{s/\pi}$ (see Fig. 1). In addition, the moment of inertia was numerically calculated by the formula [7]

$$I = \oiiint\limits_v (x^2 + y^2)\rho_s \, dv, \tag{2}$$

where ρ_s and v are, respectively, the density and volume of a needle or thin twig.

The midsection areas s of the CFM elements were determined as functions of their heights h obtained from photographs of needle cross sections at 20-fold magnification (see Fig. 2).

To estimate the accuracy of the results obtained, we made control measurements and calculations of values of f for cylinders of pine and steel. Thus, for a cylindrical sample of pine ($l_s = 72$ mm, $d_s = 5$ mm, density $\rho_s = 0.5 \cdot 10^3$ kg/m^3, and Young's modulus $E = 10^{10}$ N/m^2), the natural frequency calculated by formula (1) is $f_{\rm calc} = 861$ Hz and the measured frequency is $f = 667$ Hz. For a steel cylinder ($l = 53$ mm, $d = 1$ mm, $E = 2 \cdot 10^{11}$ N/m^2, and $\rho = 7800$ kg/m^3), $f_{\rm calc} = 365$ Hz and $f = 312$ Hz. The values of E are taken from [8]. Obviously, the experimental data agree well with the calculated results.

Table 4 gives values of the elastic characteristics of typical CFM elements. A comparison of the results obtained to the well-known data validates the proposed method for determining the elastic properties of CFM. The confidence intervals ΔE were calculated from the results of 4 or 5 experiments at a confidence probability of 0.95.

5. Results of Studying Oscillations in a Twig–Needle System. Figure 3d and e shows typical oscillograms of the transverse displacement of a needle. Figure 3d (see the diagram in Fig. 1c) and Fig. 3e (see the diagram in Fig. 1d) correspond to $u_\infty = 1.1$ m/sec. Table 5 gives typical oscillation frequencies and amplitudes for various experimental conditions. Table 6 gives oscillation frequencies and amplitudes for the experimental conditions corresponding to the diagram shown in Fig. 1e (see also Fig. 3e).

TABLE 4

CFM element	f, Hz	m, g	l_s, mm	d_s, mm	W, %	E_{eff}, N/m^2	EI, N · m^2
Fir needle	4.4	2.1	16	0.7	11.3	$(0.94 \pm 0.03) \cdot 10^7$	$2.24 \cdot 10^{-7}$
Cedar needle	38.5	4.8	80	1.0	10.8	$(0.78 \pm 0.05) \cdot 10^9$	$7.65 \cdot 10^{-5}$
Pine needle	21.4	2.9	41	0.9	16.2	$(3.24 \pm 0.07) \cdot 10^{10}$	$4.11 \cdot 10^{-4}$
Pine needle	16.7	4.6	43	1.0	34.9	$(1.79 \pm 0.06) \cdot 10^{10}$	$7.2 \cdot 10^{-4}$
Pine needle	20.0	5.4	43	0.9	67.8	$(0.85 \pm 0.05) \cdot 10^{10}$	$5.47 \cdot 10^{-4}$
Pine twig	2.1	3.6	60	4.0	—	$(0.89 \pm 0.02) \cdot 10^{10}$ $(0.9 \cdot 10^{10})^*$	0.22

Asterisk denotes that the value of E is given for cylinders of wood [8].

TABLE 5

u_∞, m/sec	Fig. 1c			Fig. 1d		
	A, mm	f_1, Hz	f_2, Hz	A, mm	f_1, Hz	f_3, Hz
1.1	1.15	20–26	—	1.30	20–25	5–6
1.6	1.56	18–22	40–46	—	—	—
1.9	1.74	18–22	40–42	—	—	—
2.5	1.91	20–25	39–41	—	—	—
3.1	2.07	20–26	40–41	1.41	19–25	5–6
3.6	2.20	20–25	40–45	1.50	20–26	5–5

Note. The frequency f_3 is absent in the experiments according to the diagram in Fig. 1c and the frequency f_2 is absent in the experiments according to the diagram in Fig. 1d.

TABLE 6

u_∞, m/sec	Twig–Needle System			
	A', mm	f', Hz	A'', mm	f'', Hz
1.1	0.40	2.0	0.75	60–70
1.6	0.45	2.0	0.89	62–70
1.9	0.46	2.1	0.99	58–67
2.5	0.52	2.1	1.39	60–70
3.1	0.58	2.1	1.52	65–70
3.6	0.62	1.9	1.70	60–70

Note. One prime and two primes corresponds to the twig and needle, respectively.

An analysis of the results given in Fig. 3 and Tables 4 and 5 shows that only three dominant frequencies are available in the spectra of oscillations of the twig–needle system: $f_1 = 18$–25 Hz, $f_2 = 40$–46 Hz, and $f_3 = 5$–6 Hz. With increase in flow rate, the oscillation amplitude increases monotonically, while the frequency remains almost unchanged. The natural frequency of the CFM elements depends only slightly on the flow rate because this frequency is a function of geometrical dimensions, mass, and elastic properties of twigs and needles [1, 7].

At a flow rate of $u_\infty \approx 1.5$ m/sec, oscillations of the twig at a frequency $f_2 \approx 2f_1$ are imposed on the oscillations of the needle (see Fig. 1 *d*). We note that the displacement of the needle end along the x axis due to oscillations of the twig is always positive. From an analysis of the experimental data, this can be explained by deformation of the CFM elements due to the velocity head of the air flow. The measured oscillation frequency of the base of the needle (end of the twig) $f = 36$–42 Hz is close to the values of f_2, and this confirms the mechanism of oscillations with frequency f_2.

For the flow around the twig–needle system according to the diagram in Fig. 1c, modulation of transverse oscillations of the needle occurs for a flow rate of $u_\infty \geqslant 1.1$ m/sec (see Fig. 4d). The frequency of the modulating oscillations $f_3 = 5$–6 Hz, as well as the oscillation frequency of needles, practically do not depend on the flow rate. The modulation results from superposition of transverse oscillations of the needle and longitudinal oscillations of the twig (see Fig. 1b). This was confirmed by measuring the oscillation frequencies of the base of the needle (twig end) ($f = 5$–8 Hz).

The twig–needle system is sensitive to acoustic vibrations generated by a dynamic speaker and an audio oscillator [3]. The intensity of sound was 60 dB, and the frequency of harmonic oscillations was varied from 10 to 100 kHz. At frequencies of $f = 10$–100 Hz, the oscillations of needles and twigs were insensitive to acoustic vibrations, and at frequencies of 1–50 kHz, the modulating frequency "smeared" up to complete attenuation (see Fig. 3c). Such frequencies of ultrasonic vibrations are close to the natural frequencies of longitudinal oscillations of the CFM elements. The attenuation of oscillations with a modulating frequency of $f = 5$–6 Hz is probably related to a change in elastic properties of the CFM elements due to resonance phenomena.

6. Effect of Oscillations of the Twig–Needles System on Combustion Process. Resonance phenomena affect the burning of the twig–needles system in the case of longitudinal (along the Ox axis) oscillations of the base of the needle (see Fig. 1e). In the experiments, the oscillation frequency f varied within the range of $0 \leqslant f \leqslant 6.2$ Hz and the amplitudes were $\delta x = 0$–14 mm. A twig with needles was ignited and, depending on the oscillation intensity, we observed its burning or extinguishing. During the experiments, the heat flux density q in the combustion zone was recorded by an exponential method [1, 3] using a total heat flux sensor.

Calculations of the dependence of the relative function of heat exchange

$$\Psi_{\text{oscill}} = (q_+ - q_-)/q_-, \tag{3}$$

where q_+ and q_- are, respectively, the heat flux densities in the burning zone with and without oscillations of the twig with needles ($q_- = 3.2 \cdot 10^4$ W/m^2) versus the oscillation Reynolds number $\text{Re}_{\text{oscill}} = v_{\text{oscill}} d/\nu$ [$v_{\text{oscill}} = (\delta x) f$ and $\nu = 1.45 \cdot 10^{-5}$ m^2/sec is the kinematic viscosity of air], give the following results: $\Psi_{\text{oscill}} = 0$, 0.15, 0.25, 0.56, and 0 for $\text{Re}_{\text{oscill}} = 0$, $4.9 \cdot 10^3$, $7.8 \cdot 10^3$, $13.1 \cdot 10^3$, and $15.0 \cdot 10^3$, respectively.

These data show that up to Reynolds numbers $\text{Re}_{\text{oscill}} = 13.1 \cdot 10^3$, the system ($\Psi_{\text{oscill}} > 0$) ignites and burns, while at $\text{Re}_{\text{oscill}} > 13.1 \cdot 10^3$, the flame extinguishes, and the oscillation frequency $f = 2.1$ Hz corresponds to the natural frequency of the twig. Resonance is responsible for an increase in the oscillation amplitude of the system and, hence, flameout and extinction.

7. Analysis of the Results. It has been shown previously [1] that at the front of an upper forest fire, CFM burns in a diffusive regime. Therefore, under certain conditions, mechanical oscillations of needles and thin twigs can increase heat or oxygen inflow to them during ignition of a needle in the forest canopy, and, as a result, the burning rate of CFM increases. However, if the wind speed is very high, burning of CFM can stop because of large heat losses due to interaction of the elementary torch (tongue) surrounding a burning element with a relatively cold air flow. This follows both from the results described in Sec. 6 and from experimental data on ignition of fresh needles and twigs with needles of cedar, fir-tree, and pine (see [2, Tables 1.14 and 1.15]). The aforesaid agrees well with the theoretical results discussed in [1], where it is shown that there are lower and upper limits for propagation of an upper forest fire with respect to the wind speed.

From the results shown in [4, 5] and the above experimental data, it follows that the mechanism of oscillations of the CFM elements, namely, needles and thin twigs, agrees well with the mechanism proposed in [1, p. 152, 153].

According to [1], in a forest canopy, the so-called equilibrium wind speed $u_{*\infty}$ is established in the absence of a fire, which differs from the unperturbed wind speed u_∞ in the ground atmospheric layer. Thus, for further analysis we used the value of $u_{*\infty}$. The value of the equilibrium wind speed $u_{*\infty} = 2.2$ m/sec obtained in [1] for a needle can be regarded as the lower limit for an upper forest fire. This value agrees with the results of semi-natural experiments [9], during which it was found that in a pine underwood a lower forest fire becomes an upper fire only at a wind speed of 3 m/sec.

8. Conclusions. An experimental procedure for studying oscillations of the elements of forest combustible materials was developed using optoelectronic equipment in a laminar air flow. A comparison of the experimental data with the theoretically derived frequencies of sample cantilevers of steel and pine wood showed that the error in determining amplitudes and frequencies of natural and forced oscillations is 15–22%.

Based on the experimental data on the minimum oscillation frequencies and formula (1), a method of determining Young's modulus E and the rigidity EI for needles and thin twigs was constructed. The values of E and EI were obtained for pine, cedar, and fir needles. For cedar needles, it was found that the values of E and EI decrease with increase in moisture content.

It was established experimentally that interaction of the CFM elements with the air flow leads to asymmetric separation of the flow, which, in turn, makes needles and twigs oscillate at a frequency of $f = 18$–25 Hz. This frequency depends weakly on the flow rate and is equal to the natural frequency. An increase in the flow rate results in an increase in the oscillation amplitude and can lead to further turbulization of the air flow in the vicinity of the CFM elements. It was proved that over the spectra of oscillation frequencies, the effects of amplitude modulation of the resulting oscillations can arise due to the oscillations of the twig–needles system.

REFERENCES

1. A. M. Grishin, *Mathematical Modeling of Forest Fires and New Methods of Fire Fighting* [in Russian], Nauka, Novosibirsk (1992).
2. A. M. Grishin, *Physics of Forest Fires* [in Russian], Izd. Tomsk. Univ., Tomsk (1994).
3. A. M. Grishin and A. N. Golovanov, "On the effect of small acoustic perturbations on the drying, pyrolysis, and ignition of combustible forest materials," *Sib. Fiz.-Tekh. Zh.*, **6**, 102–106 (1992).
4. A. A. Zhukauskas, *Convective Transfer in Heat and Mass Exchangers* [in Russian], Nauka, Moscow (1982).
5. E. Smiu and R. Scanlan, *Wind Effect on Structures: An Introduction to Wind Engineering*, John Wilew and Sons, New York.
6. J. P. Den Hartog, *Mechanical Vibrations*, McGraw-Hill, New York, etc. (1956).
7. L. D. Landau and E. M. Lifshits, *Mechanics of Continuous Media* [in Russian], Gostekhteoretizdat, Moscow (1953).
8. B. N. Ugolev, *Dendrology with Foundations of Timber Commodity Research* [in Russian], Lesnaya Promyshlennost', Moscow (1975).
9. A. M. Grishin, V. E. Abaltusov, A. I. Vesnin, et al., "Experimental studies of the spread of upper forest fires and heat transfer of a fire front with the environment," Tomsk. Univ. (1982). Deposited at VINITI 09.03.82, No. 4873-82.